An RNA motif advances transcription by preventing Rho-dependent termination

Anastasia Sevostyanova[a,b] and Eduardo A. Groisman[a,b,c,1]

[a]Howard Hughes Medical Institute, Yale School of Medicine, New Haven, CT 06536; [b]Department of Microbial Pathogenesis, Yale School of Medicine, New Haven, CT 06536; and [c]Microbial Sciences Institute, Yale University, West Haven, CT 06516

Edited by Jeffrey W. Roberts, Cornell University, Ithaca, NY, and approved October 15, 2015 (received for review August 3, 2015)

The transcription termination factor Rho associates with most nascent bacterial RNAs as they emerge from RNA polymerase. However, pharmacological inhibition of Rho derepresses only a small fraction of these transcripts. What, then, determines the specificity of Rho-dependent transcription termination? We now report the identification of a Rho-antagonizing RNA element (RARE) that hinders Rho-dependent transcription termination. We establish that RARE traps Rho in an inactive complex but does not prevent Rho binding to its recruitment sites. Although translating ribosomes normally block Rho access to an mRNA, inefficient translation of an open reading frame in the leader region of the *Salmonella mgtCBR* operon actually enables transcription of its associated coding region by favoring an RNA conformation that sequesters RARE. The discovery of an RNA element that inactivates Rho signifies that the specificity of nucleic-acid binding proteins is defined not only by the sequences that recruit these proteins but also by sequences that antagonize their activity.

Rho-dependent termination | antitermination | *Salmonella* | MgtC | transcriptional polarity

Transcription factors recognize sequence and structural elements in DNA and RNA to turn genes on or off. The transcription termination factor Rho is responsible for the majority of factor-dependent termination events in enteric bacterial species (1). Rho prevents the production of dysfunctional, and potentially dangerous, RNAs (2). For instance, Rho implements transcriptional polarity, a process whereby compromised translation of a promoter-proximal gene reduces transcription of downstream genes in an operon (3–5).

Rho is a hexameric helicase that binds RNA and translocates in the 5′-to-3′ direction using the energy derived from ATP hydrolysis. Initially, RNA is anchored to Rho primary binding sites on the surface of the hexamer. Rho recruitment sites tend to be rich in Cs and Us and free of strong secondary structures (6–8). Interaction with a recruitment site causes the Rho hexamer to open briefly, allowing the RNA 3′ region to pass through the center, where secondary binding sites are located (9, 10). Further contact between the RNA and the secondary binding sites stimulates Rho's ATPase activity (11). Using the energy derived from ATP hydrolysis, Rho translocates along an RNA until it reaches a paused RNA polymerase (RNAP) and promotes transcription termination (12).

The specificity of Rho-dependent transcription termination has remained enigmatic because Rho associates with many newly transcribed RNAs in *Escherichia coli* (13), but only a portion of these messages is affected when bacteria are treated with bicyclomycin (BCM) (1), a Rho-specific inhibitor (14). In other words, binding of Rho to a particular RNA is not sufficient for subsequent transcription termination.

Rho-dependent terminators are typically found at the end of operons; however, they can also be present in the leader region of mRNAs, where they perform regulatory functions (15–17). This appears to be the case for the 296-nt-long leader region of the *mgtCBR* transcript from *Salmonella enterica* serovar Typhimurium, which controls transcription elongation into its associated coding region (18, 19) but lacks sequences that resemble an intrinsic terminator [i.e., a G + C-rich stem-loop followed by a stretch of Us (12)]. The *mgtCBR* operon specifies the virulence protein MgtC (20), the Mg^{2+} transporter MgtB (21), and the regulatory peptide MgtR (22).

We now report the identification of a Rho-antagonizing RNA element (RARE) in the *mgtCBR* leader that prevents transcription termination by factor Rho. We establish that RARE traps Rho in a nonfunctional state (as opposed to hindering Rho binding to its recruitment sites), and we define the sequences and positions governing RARE activity. In contrast to transcriptional polarity, wherein a translating ribosome protects RNA from Rho invasion (12), translation of a short open reading frame (ORF) in the *mgtCBR* leader actually compromised RARE action, thereby preventing transcriptional readthrough into the associated coding region. Our findings indicate that the arrangement of genetic elements governing Rho activity, rather than simply the coupling of transcription and translation, determines how translation of an upstream ORF influences downstream transcription. Furthermore, they imply that nucleic-acid binding proteins manifest specificity both by sequences that recruit these proteins and by sequences that hinder their function.

Results

The *mgtCBR* Leader Harbors a Rho-Dependent Transcription Terminator. We determined that the *mgtCBR* leader includes a Rho-dependent terminator because the mRNA levels of the *mgtC* coding region increased sixfold when bacteria were treated with the Rho-specific inhibitor BCM (Fig. 1*A*). To identify the site of transcription termination in the *mgtCBR* leader, we carried out single-round in vitro transcription assays with purified RNAP and a DNA template that contained the λP_R promoter and a 26-nt long C-less region

Significance

Transcription factors typically bind to more sites than are functionally affected upon transcription factor inactivation. What, then, determines whether transcription factor binding impacts gene expression? Here we address this question by investigating Rho, the essential transcription termination factor that associates with most newly transcribed RNAs in bacteria, but promotes transcription termination only in a fraction of these transcripts. We uncover a novel RNA element that sequesters Rho in an inactive complex, thereby advancing transcription without affecting Rho binding. Our results indicate that the site of action of transcription factors is defined not only by sequences that mediate their recruitment but also by sequences that antagonize their activity.

Author contributions: A.S. and E.A.G. designed research; A.S. performed research; A.S. and E.A.G. analyzed data; and A.S. and E.A.G. wrote the paper.

The authors declare no conflict of interest.

This article is a PNAS Direct Submission.

[1]To whom correspondence should be addressed. Email: eduardo.groisman@yale.edu.

This article contains supporting information online at www.pnas.org/lookup/suppl/doi:10.1073/pnas.1515383112/-/DCSupplemental.

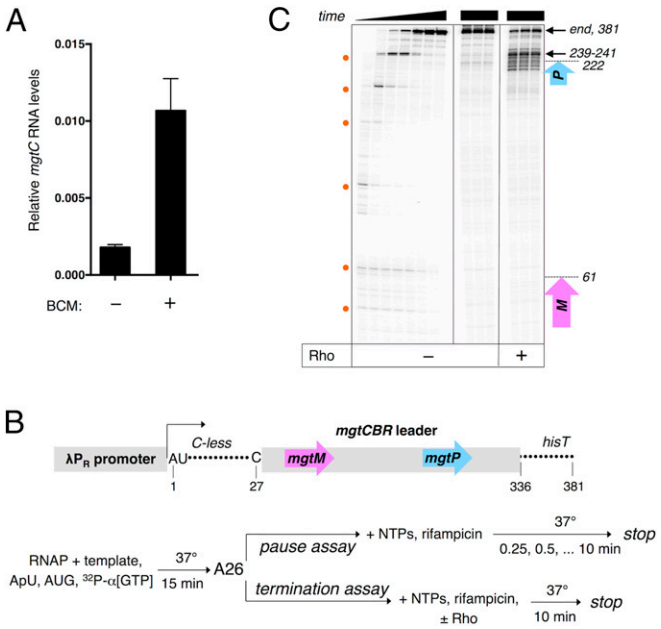

Fig. 1. The *mgtCBR* transcript harbors a Rho-dependent transcription terminator within its leader. (*A*) The Rho-specific inhibitor BCM derepresses *mgtC* transcription in vivo. mRNA levels of the *mgtC* coding region produced by wild-type *Salmonella* (14028s) in the presence or absence of BCM as determined by qRT-PCR. Cells were harvested after 3 h of growth in N-minimal medium with 10 μM Mg^{2+} followed by a 15-min treatment with BCM. Shown are the mean and SD from at least three independent experiments. (*B*) Schematic of the linear DNA template and experimental strategy used in the pause and termination assays. (*C*) A representative 6% denaturing gel of pause and termination assays performed as described in (*B*). Pause assay is shown (*Left*) and positions of pause sites are indicated by the orange dots. Termination assay performed in triplicate is shown in the next three panels. Positions of the pause sites and termination products mapped in the presence of chain-terminating NTPs are indicated on the *Right* (*Materials and Methods*). The purple and blue arrows show the positions of the *mgtM* and *mgtP* ORFs located in the *mgtCBR* leader.

followed by the sequence corresponding to the *mgtCBR* leader (Fig. 1*B*). On this template, transcription elongation complexes halted by the omission of CTP can resume transcription upon addition of all four NTPs.

We detected bands that faded away over time (Fig. 1*C*), which correspond to RNA products of RNAPs pausing at several sites until they reach the end of the template. In the absence of Rho, the majority of the RNAPs reached the end of the template (Fig. 1*C*), supporting the notion that the *mgtCBR* leader lacks an intrinsic transcription terminator. Addition of Rho to the in vitro transcription reaction gave rise to prematurely terminated RNA products (Fig. 1*C*). The 3′ ends of these termination products were distributed from positions 130–290 relative to the transcription start site, with the strongest termination site located at positions 239–241 (Fig. 1*C*). This site corresponds to the most prominent pause site in the *mgtCBR* leader (Fig. 1*C*), consistent with Rho preferentially inducing RNA release from paused elongation complexes (12). Together, these results demonstrate that the *mgtCBR* leader contains a Rho-dependent transcription terminator.

The Conformation of the *mgtCBR* Leader Dictates Rho-Dependent Termination. The *mgtCBR* leader harbors two short ORFs, *mgtM* and *mgtP*, within or immediately adjacent to sequences with the ability to adopt alternative stem-loop structures (Figs. 1*B* and 2*A*) (18, 19). Mutations favoring one of these structures (i.e., stem-loop A) advance transcription into the coding region, whereas those furthering the alternative structure (i.e., stem-loop B) promote transcription termination within the *mgtCBR* leader (Fig. 2*A*) (18). We investigated the ability of Rho to terminate transcription in *mgtCBR* leader variants genetically locked in the stem-loop A or B conformations. The G54C substitution, which hinders formation of stem-loop A (Fig. 2*A*) (18), increased Rho-dependent termination in vitro (Fig. S1*A*). By contrast, the G95C substitution, which prevents formation of stem-loop B (Fig. 2*A*), reduced the fraction of prematurely terminated products (Fig. S1*A*). We concluded that stem-loops A and B exert their regulatory effects directly by influencing Rho's ability to terminate transcription in the absence of any additional factors.

A Rho Recruitment Site Is Necessary for Transcription Termination in the *mgtCBR* Leader. Transcription termination by Rho occurs in several steps, beginning with Rho binding to a *rut* (Rho utilization) site in a transcript (2, 23, 24). We identified a potential *rut* site immediately downstream of stem-loop B (Fig. 2*A*). Substitution of nucleotides in this region (positions 105–125) dramatically increased transcription of the associated coding region in vivo (Fig. 2*B*, [105–125]), and this was also the case when only four C residues were substituted by AUGU (Fig. 2*B*, [109–112]), indicating that the identified region functions as an authentic *rut* site. By contrast, deletion of nucleotides upstream and downstream of this site had no effect on transcription elongation into the coding region (Fig. 2*B*, Δ65–70, Δ71–78, Δ128–154, and Fig. S2*A*).

The increased transcription resulting from nucleotide substitutions in the *rut* site is due to diminished Rho-dependent termination. This is because BCM addition to cells harboring a leader mutated in the Cs at positions 109–112 increased the mRNA levels of the associated coding region only threefold, significantly less than the 16-fold increase BCM promoted in the isogenic strain with the wild-type leader (Fig. 2*C*). Moreover, the [105–125] RNA variant stimulated Rho's ATPase activity much less than the wild-type leader RNA (Fig. 3*A*), indicating that this region is required for Rho function (Rho's ATPase activity reflects both Rho loading and subsequent translocation on its RNA substrate).

To evaluate the contribution of individual nucleotides within and around the identified *rut* site on transcription termination, we used a variant of the *mgtCBR* leader locked in a conformation favoring Rho recruitment (Fig. 2 *A* and *B*, Δstem B). This allowed us to refine the borders of the *rut* site to positions 108–131 (Fig. S2*B*). With the exception of the C119G substitution, single nucleotide substitutions of the Cs or Us in the 108–131 region displayed only a modest increase in expression of the associated coding region (Fig. S2*B*). These results are consistent with the premise that Rho recruitment relies on multiple nonspecific and sequence-specific contacts in RNA spread out over a large segment of a transcript (2, 23, 24). Structural probing of an RNA fragment corresponding to the wild-type *mgtCBR* leader with lead acetate revealed small but distinct changes in sensitivity within the identified *rut* region upon addition of Rho (Fig. S2*C*). Cumulatively, these data identified a region of the *mgtCBR* leader mRNA critical for Rho-dependent transcription termination.

RARE Inhibits Rho-Dependent Termination When Not Sequestered in a Hairpin. Leader RNAs that harbor Rho-dependent transcription terminators often have the ability to adopt mutually exclusive conformations, one favoring and one hindering the ability of Rho to terminate transcription. For example, a *rut* site is sequestered within a stem in the *mgtA* leader conformer hindering Rho-dependent termination, but single stranded and available to Rho in the conformer that favors Rho-dependent termination (15). By contrast, the *rut* site identified in the *mgtCBR* leader is single stranded in both the stem-loop A and B conformations (Fig. 2*A*), which prevent and stimulate Rho activity, respectively (Fig. S1). What, then, determines Rho recruitment and transcription termination in the *mgtCBR* leader?

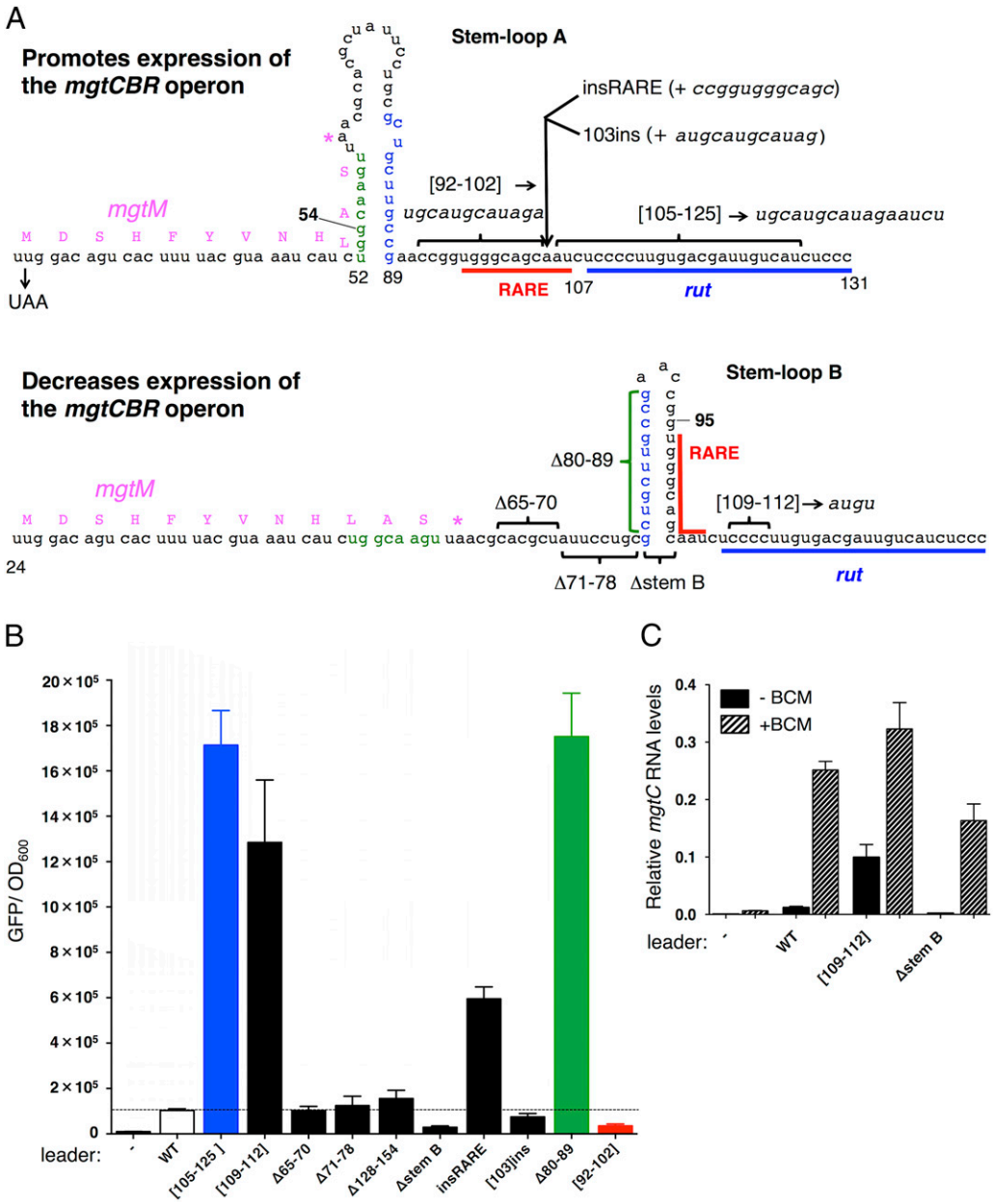

Fig. 2. RARE prevents Rho-dependent termination in the *mgtCBR* leader RNA. (*A*) Schematic of two alternative conformations that the 5′ end of the *mgtCBR* leader RNA can adopt (18). Positions of insertions are indicated by arrows, deletions and substitutions by brackets, and mutations that selectively destabilize stem-loops A and B by numbers in bold face. The calculated ΔG values for stem-loops A and B are −14.8 kcal/mole and −17.8 kcal/mole, respectively. (*B*) Fluorescence levels exhibited by wild-type *Salmonella* (14028s) harboring a plasmid that contains a transcriptional fusion between the wild-type *mgtCBR* promoter and leader, or *mgtCBR* leader variants, to a promotorless *gfp* gene. (–) corresponds to wild-type *Salmonella* (14028s) harboring the plasmid vector pFPV25. Shown are the mean and SD from at least three independent experiments. (*C*) *gfp* mRNA levels produced by wild-type *Salmonella* (14028s) harboring a plasmid with a transcriptional fusion of the wild-type *mgtCBR* promoter and leader, or *mgtCBR* leader variants with the Cs at positions 109–112 substituted by AUGU, or deleted for nucleotides 79–103 (ΔstemB), to a promotorless *gfp* gene. mRNA levels were determined by qRT-PCR. Cells were harvested after 3 h growth in N-minimal medium with 10 μM Mg^{2+} followed by a 15-min treatment with BCM. (–) corresponds to wild-type *Salmonella* (14028s) harboring the plasmid vector pFPV25. Shown are the mean and SD from at least three independent experiments.

We hypothesized that nucleotides 92–102 regulate Rho-dependent transcription termination because these nucleotides are single stranded when the leader forms stem-loop A but double stranded when the leader folds into stem-loop B (Fig. 2*A*). We designated this region RARE for Rho-antagonizing RNA element. If stem-loop B promotes transcription termination by sequestering RARE, then rendering RARE single-stranded should overcome the inhibitory effect of stem-loop B on transcriptional readthrough. As hypothesized, expression of the associated coding region increased sixfold when a second copy of RARE was inserted after stem-loop B (Fig. 2 *A* and *B*, insRARE), but not when a random sequence of the same length was inserted at the identical position (Fig. 2 *A* and *B*, [103]ins).

Several lines of evidence provide additional support to the notion that a single-stranded RARE hinders termination by Rho within the *mgtCBR* leader. First, removing the left arm of stem-loop B (i.e., positions 80–89, Fig. 2*A*), which rendered RARE single stranded, increased expression of the coding region 17-fold (Fig. 2*B*, Δ80–89). We ascribe the increased expression of the

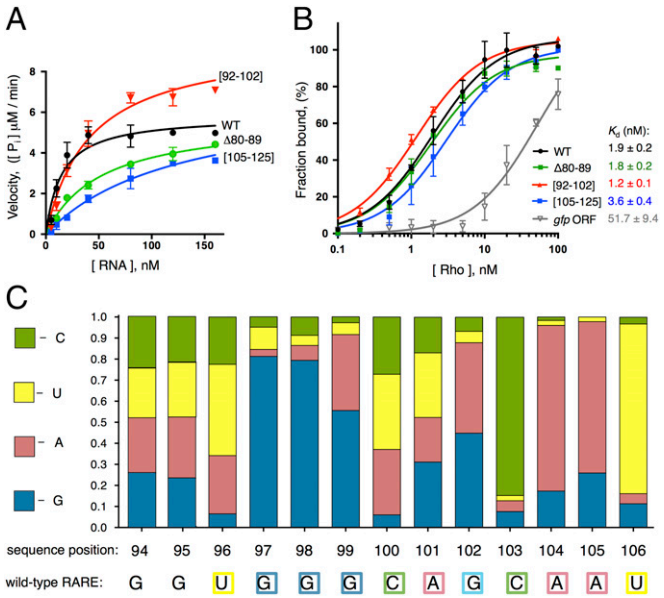

Fig. 3. RARE traps Rho in a catalytically inactive complex. (*A*) Stimulation of Rho's ATPase activity by the wild-type *mgtCBR* leader RNA or three variants (Fig. 2*A*). ATPase activity was measured by monitoring the accumulation of free phosphate with increasing concentrations of RNA (15). Each data point is an average of at least three independent experiments. (*B*) RARE does not affect Rho binding to the *mgtCBR* leader RNA. A ^{32}P-labeled fragment of the wild-type *mgtCBR* leader RNA, its mutant variants or control RNA corresponding to the 3′ region of the *gfp* ORF was incubated with increasing concentrations of Rho, and protein-bound RNA fractions were separated by filtering. The amount of filter-bound ^{32}P-RNA was plotted against the concentration of Rho, and an apparent K_d was determined by fitting data to a hyperbolic equation. Each data point is an average of at least three independent experiments. (*C*) Relative activity of RARE variants with single nucleotide substitutions at each of the positions. All mutants were derived from an *mgtCBR* leader variant lacking nucleotides 80–89 to lock RARE in a single-stranded form. Fluorescence values produced by wild-type *Salmonella* (14028s) harboring a plasmid that contains a transcriptional fusion between the wild-type *mgtCBR* promoter and the Δ80–89 *mgtCBR* leader variant with single nucleotide substitutions at each position of RARE to a promotorless *gfp* gene were summed up and set as 1. The colored segments of each bar represent relative activity of RARE containing G, A, U, or C at a given position. The wild-type RARE sequence is indicated below. Bacteria were grown as described in the legend to Fig. 2*B*.

latter mutant to impaired Rho function because the corresponding RNA stimulated Rho's ATPase activity significantly less than did the wild-type RNA (Fig. 3*A*). This means that RARE exerts its antitermination effect specifically by impairing Rho function and not by modifying RNAP or recruiting a cellular cofactor. Second, replacement of RARE by a scrambled sequence promoted Rho-dependent termination in vivo (Fig. 2*B*, [92–102]), and, as expected, the corresponding RNA stimulated Rho's ATPase activity more than the wild-type leader RNA in vitro (Fig. 3*A*). These results indicate that the removal of RARE from the *mgtCBR* leader makes the resulting RNA a better substrate for Rho. This result is despite the fact that the mutation prevented formation of stem-loop B. And third, removal of stem-loop B (i.e., positions 79–103, Fig. 2*A*) reduced transcription of the associated coding region to near background levels (Fig. 2*B*, Δstem B), like the mutant with the scrambled RARE. The silencing effect resulting from removal of stem-loop B is due to Rho activity because addition of BCM to cells harboring this variant increased the mRNA levels of the associated coding region 40-fold (Fig. 2*C*, Δstem B), significantly more than the increase observed in the isogenic strain with the wild-type *mgtCBR* leader (16-fold, Fig. 2*C*) or in the strain with a mutation in the *rut* site (threefold, Fig. 2*C*, [109–112]). We conclude that single-stranded RARE directly prevents Rho from terminating transcription in the *mgtCBR* leader, thereby allowing elongation into the associated coding region.

Rho Binds Normally to *mgtCBR* Leader Variants with RARE Single Stranded or with a Mutant *rut*. The selectivity of Rho-dependent termination has been ascribed to the initial binding of Rho to its RNA substrate (2). However, we have now established that RARE exerts its regulatory effect after the initial binding of Rho, arguing against this notion. That is, Rho bound with a high affinity to the leader variant with RARE single stranded, similar to that exhibited toward the wild-type *mgtCBR* leader RNA (Fig. 3*B*, apparent K_d = 1.8 ± 0.2 nM, Δ80–89 versus 1.9 ± 0.2 nM, WT), and only slightly better to an RNA lacking RARE (Fig. 3*B*, apparent K_d = 1.2 ± 0.1 nM, [92–102]). By contrast, Rho bound with ∼30-fold lower affinity to a control RNA segment of the same length originating from the *gfp* coding sequence (Fig. 3*B*, apparent K_d = 51.7 ± 9.4 nM, *gfp* ORF).

Surprisingly, Rho's affinity for the RNA with mutations in the *rut* was only twofold lower than that of the wild-type *mgtCBR* leader RNA (Fig. 3*B*, apparent K_d = 3.6 ± 0.4 nM, [105–125] versus 1.9 ± 0.2 nM, WT) even though this mutation led to dramatic derepression in vivo (Fig. 2*B*, [105–125]). The modest decrease in affinity displayed by the RNA with mutations in a *rut* in the *mgtCBR* leader is in contrast to the effect of mutation of a *rut* site in the *mgtA* leader region (15, 25), which decreased affinity for Rho eightfold [Fig. S3*A*, apparent K_d = 2.6 ± 0.3 nM for the C145G *mgtA* variant promoting an RNA conformation favorable for Rho binding (15) versus 20.1 ± 2.6 nM for the R1 variant with substitutions in a *rut* site (15)]. Nevertheless, extensive deletion analysis revealed that nucleotides in the [105–125] region were the only ones required for Rho-dependent termination within the 5′ half of the *mgtCBR* leader (Fig. 2*B*, compare [105–125] and [109–112] to Δ65–70, Δ71–80, ΔstemB, Δ128–154, and Fig. S2*B*, compare [109–112] to Δ4–10, Δ11–16, Δ17–23, Δ24–38, Δ39–50, and Δ51–60), suggesting that this region serves as a genuine *rut* site. Cumulatively, our findings revealed two distinctive features of Rho interaction with the *mgtCBR* RNA. First, RARE exerts its inhibitory activity after the initial Rho binding takes place and in the absence of any additional cellular factors. And second, the role of the identified *rut* site is to stimulate Rho's activity after binding rather than simply to tether the RNA to Rho.

The Sequences and Positions Required for RARE Activity. To define the RARE residues hindering Rho-dependent transcription termination, we mutated each of the 13 nucleotides within the 94–106 region to each of the other three. We used as parental template a leader variant deleted for nucleotides 80–89 so that RARE would always be single stranded, and thus available to inhibit Rho (Fig. 2*A*). Then, we measured the fluorescence produced by wild-type *Salmonella* harboring a plasmid with a transcriptional fusion between the wild-type *mgtCBR* promoter and the *mgtCBR* leader variant lacking nucleotides 80–89, and a promotorless *gfp* gene.

We established that G97, G98, C103, A104, and U106 are the most important RARE residues because substitutions at these positions to any other nucleotide severely decreased fluorescence (Fig. 3*C* and Fig. S3*A*). Mutations at positions 99 and 102 had different effects depending on the substituting nucleotide. For example, the G102A mutant retained the parental behavior, whereas substitution of G102 to U or C decreased fluorescence six- to eightfold (Fig. 3*C* and Fig. S3*A*). This result suggests that G102 is involved in wobble base pairing with a U residue that may also establish a canonical base pair with A, but not with U or C. Mutations at positions 100 and 101 actually increased fluorescence, suppressing transcription termination even more efficiently than the parental RARE (Fig. S3*A*). Finally, substitutions

at positions 94 and 95 did not have detectable effects on fluorescence (Fig. 3*C*).

How do the identified RARE nucleotides affect termination by Rho? In silico secondary structure predictions raised the possibility of stem-loops forming between RARE residues and the adjacent *rut* nucleotides (Fig. 4*A*). Analysis of compensatory mutations within *rut* (Fig. S4*A*) that restored activity of RARE with single-nucleotide substitutions provided evidence of limited base-pairing interaction between these regions (e.g., G102–U125, C103–G124, and A104–U123; Fig. 4*B* and Fig. S4*A*). However, no interactions between Gs at positions 97–99 and the CU-rich motif at 128–131, which would form the base of a hypothetical stem-loop, were observed (Fig. 4 *A* and *B*). The only putative base pair identified by a compensatory mutation analysis (C97–C129) is incompatible with the in silico model (Fig. 4 *A* and *B*), and the remaining interactions appear insufficient to form a stable secondary structure (Fig. 4*B*).

RARE Promotes a Singular Conformation of the Rho–RNA Complex. How does RARE prevent Rho from terminating transcription? To address this question, we examined the interaction between Rho and *mgtCBR* leader RNA substrates using enzymatic probing.

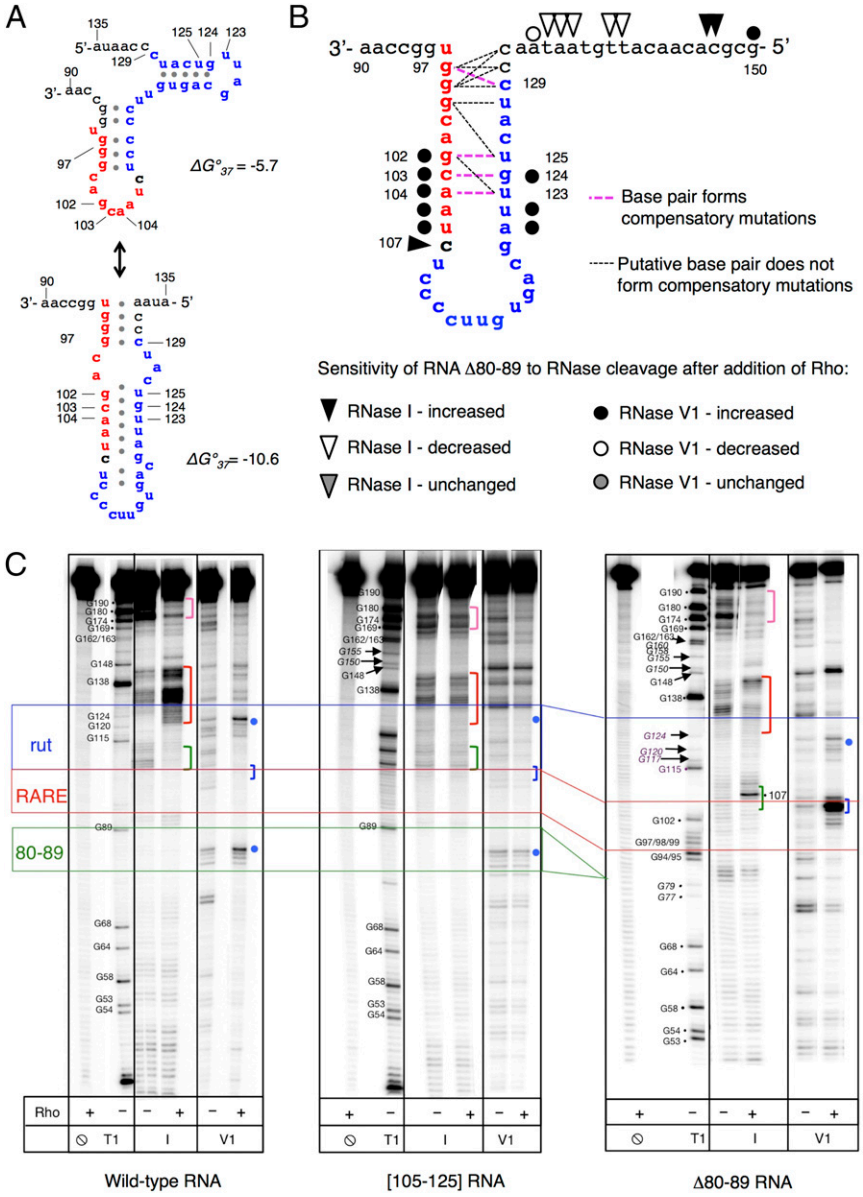

Fig. 4. RARE promotes the formation of an unusual complex between the *mgtCBR* leader RNA and Rho. (*A*) Putative secondary structures formed by RARE (red) and *rut* (blue) in the *mgtCBR* leader. Structures were generated using the Mfold web server for nucleic acid folding and hybridization prediction (46). (*B*) Graphic representation of the proposed structure formed by RARE (red) and the *rut* (blue) in the *mgtCBR* leader based on RARE mutagenesis (Fig. 3*C*), compensatory mutation analysis (Fig. S4*A*), and the structural probing shown below. Mutant combinations that restored fluorescence to the levels displayed by the Δ80–89 variant are shown in bold pink dashed lines; mutant combinations that were tested but did not restore Δ80–89 function are shown in thin black dashed lines. See text for details. (*C*) Enzymatic probing of the wild-type *mgtCBR* leader RNA and the [105–125] and Δ80–89 variants. The 5′ ^{32}P-labeled fragment of the *mgtCBR* leader RNA was treated with different RNases in the presence or absence of Rho. T1 is for RNase T1 (cuts at G residues, used as a molecular marker), I is for RNase I, and V1 is for RNase V1. Positions of interest are marked with colored dots and brackets (see text). Colored lines show borders of relevant elements: blue for *rut*, red for RARE, and green for the left arm of stem-loop B (80–89). Only the relevant lanes from a representative gel are shown. The experiment was performed at least three times for each sample.

We determined that the cleavage pattern that Rho promoted in the leader RNA with RARE single stranded (Δ80–89) differed from the patterns observed in the wild-type and the *rut* mutant variant [105–125] RNAs (Fig. 4*C*). For instance, Rho protected the wild-type *mgtCBR* leader RNA at positions 105–114 from cleavage by RNase I, an enzyme that cleaves unpaired residues (Fig. 4*C*, green bracket), but not in the *rut* mutant variant RNA (Fig. 4*C*, green bracket) even when added at saturating levels. This protected region corresponds to nucleotides required for Rho to terminate transcription (Fig. 2*B*). By contrast, Rho promoted an RNase I hypersensitive site in the Δ80–89 RNA at position 107 (Fig. 4*C*, green bracket), which is located between RARE and *rut* (Fig. 2*A*). In addition, Rho induced the appearance of RNase I hypersensitive sites at positions 130–145 in the wild-type RNA but not in the Δ80–89 RNA (Fig. 4*C*, red brackets). These results suggest that Rho promotes a conformation in the *mgtCBR* leader RNA with RARE single stranded that does not stimulate Rho's ATPase activity (Fig. 3*A*, Δ80–89).

RARE appears to contact both Rho and *rut* in the *mgtCBR* leader (Fig. 4*B*) for two reasons. First, Rho partially protected G residues within RARE in the Δ80–89 RNA from the G-specific RNase T1 (Fig. S4*B*). Second, the digestion patterns of Rho bound to the Δ80–89 RNA promoted by the RNase V1 and RNase I suggested the presence of a stem-loop structure. That is, there was an RNase V1-sensitive site at positions 103–105 (Fig. 4*C*, blue bracket) followed by RNase I-sensitive site at position 107 (Fig. 4*C*, green bracket) (RNase V1 cleaves double-stranded or stacked residues). The location of this hairpin is in excellent agreement with the model suggested by genetic analysis (Fig. 4*B*). We believe that this is a bona fide stem-loop because its RNase digestion pattern is similar to the one displayed by stem-loop B, whose presence was verified by lead acetate (Fig. S2*C*), in-line probing (18) and genetic analysis (18). In the same RNase probing assay, stem-loop B is characterized by RNase V1-sensitive site at positions 82–85, (Fig. 4*C*, blue dot, and Fig. S4*C*) followed by a site sensitive to RNase I at positions 90–92 (Fig. 4*C* and Fig. S4*C*) in the wild-type leader RNA.

Crucially, the stem-loop pattern in the Δ80–89 RNA appears only in the presence of Rho, indicating that the contacts between RARE and *rut* are unstable in the absence of Rho.

***mgtM* Translation Favors Rho-Dependent Termination in the *mgtCBR* Leader by Sequestering RARE Within a Stem.** What determines whether RARE is single stranded and allows expression of downstream genes, or sequestered within a stem and leads to premature termination within the *mgtCBR* leader? On the one hand, there are intrinsic properties of the *mgtCBR* leader RNA: stem-loop B is more stable than stem-loop A ($\Delta G^A \sim -14.8$ kcal/mole versus $\Delta G^B \sim -17.8$ kcal/mole), but stem-loop A has a kinetic advantage over stem-loop B because it emerges from the elongating RNAP before stem-loop B (Fig. 5*A*). On the other hand, a ribosome translating *mgtM* will unfold stem-loop A because the last four *mgtM* codons are embedded in stem-loop A (Fig. 2*A*). This will favor formation of stem-loop B, which will sequester RARE, resulting in transcription termination within the *mgtCBR* leader (Fig. 5*B*). By contrast, if *mgtM* translation is inefficient, stem-loop A will prevail, RARE will be single stranded, Rho will be trapped, and transcription will continue into the associated coding region (Fig. 5*C*).

According to the model described above, mutations that disrupt individual steps in the pathway should display 3′-to-5′ hierarchy when combined. In other words, mutations abolishing formation of stem-loop A should be dominant over those compromising *mgtM* translation; mutations that preclude sequestration of RARE should be dominant over those impacting RNA folding and *mgtM* translation; and mutations disrupting the Rho-binding site should be dominant over all of the above. We have now established that all these predictions are fulfilled.

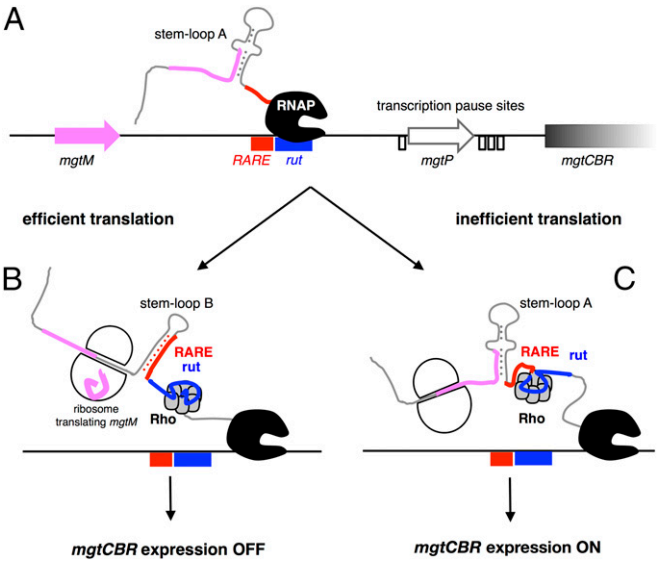

Fig. 5. Model of transcription termination control by the *mgtCBR* leader. (*A*) Schematic of the DNA region corresponding to the *mgtCBR* leader. Small ORFs are indicated by pink and white arrows; the position of RARE and *rut* are indicated by rectangles, and transcription pause sites (Fig. 2*C*) by open boxes. The leader RNA emerges from the transcribing RNAP and folds into stem-loop A. (*B*) When translation is efficient, the ribosome translating *mgtM* unwinds stem-loop A, allowing folding of stem-loop B, which sequesters RARE. Rho loads onto the RNA and translocates toward a paused RNAP. Rho triggers transcription termination, thereby turning *mgtCBR* expression OFF. (*C*) When translation is inefficient, single-stranded RARE traps Rho in an inactive state. Transcription continues, turning *mgtCBR* expression ON.

First, a mutation that abolished *mgtM* translation due to replacement of its start codon by a stop codon (Fig. 2*A*, UAA) caused a 15-fold derepression of the associated coding region (Fig. 6, UAA) but had no effect when combined with the substitution G54C (Fig. 6, UAA + G54C), which weakens stem-loop A (Fig. 2*A*, G54C) (18), or when stem-loop B was deleted (Fig. 6, UAA + Δstem B), thereby eliminating RARE (Fig. 2*A*, Δstem B). These results support the notion that a ribosome translating *mgtM* exerts its action through conformational changes in the *mgtCBR* leader RNA. Second, mutations that disrupt *mgtM* translation or favor formation of stem-loop B had little or no effect when RARE was single stranded (Fig. 6, UAA + insRARE, G54C + insRARE). These findings indicate that formation of stem-loop B and *mgtM* translation promote Rho-dependent termination in the *mgtCBR* leader by sequestering RARE. And third, substitutions in *rut* were dominant over mutations that promote formation of stem-loop B, lack RARE, or render RARE single stranded (Fig. 6, G54C + [109–112], [−RARE] + [109–112], insRARE + [109–112]). Thus, the ribosome translating *mgtM* disrupts stem-loop A, allowing sequestration of RARE in stem-loop B, leading to Rho-dependent termination within the *mgtCBR* leader.

Discussion

We have now uncovered an RNA element that sequesters termination factor Rho in an inactive complex, thereby preventing transcription termination without affecting Rho binding to its target. Rho had been known to bind preferentially to C-rich regions of RNA that are free of strong secondary structures and translating ribosomes (12). However, Rho promotes termination only at a subset of the transcripts it binds (13). The identification of RARE, an RNA motif that induces formation of a catalytically incompetent complex with Rho, indicates that Rho's specificity is defined not only by sequences that mediate its recruitment but also by sequences that antagonize its activity.

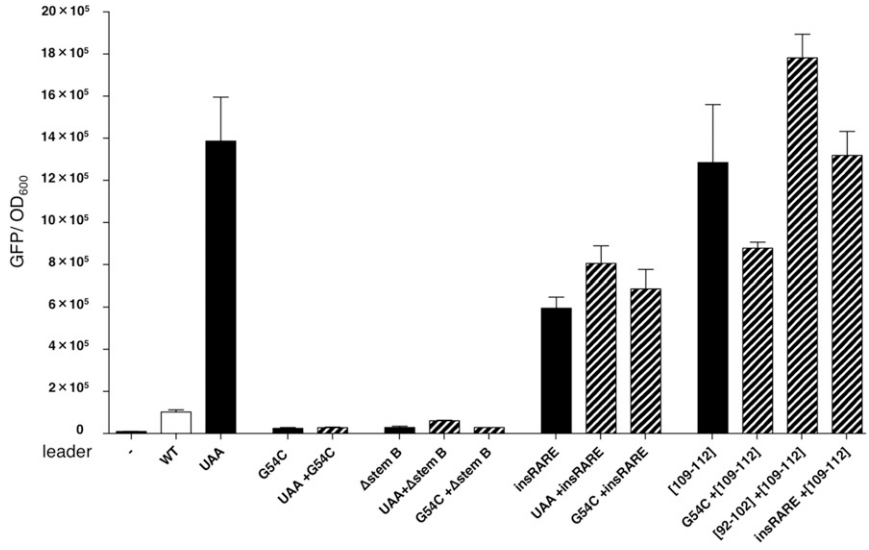

Fig. 6. *mgtM* translation promotes transcription termination by sequestering RARE. Epistasis analysis of mutations affecting Rho-dependent termination in the *mgtCBR* leader. Fluorescence levels exhibited by wild-type *Salmonella* (14028s) harboring a plasmid that contains a transcriptional fusion of the wild-type *mgtCBR* promoter and leader, or *mgtCBR* leader variants, to a promotorless *gfp* gene. The experiment was performed as described in the legend to Fig. 1*B*. Single mutations are shown with solid bars and double mutations are shown with dashed bars. (–) corresponds to wild-type *Salmonella* (14028s) harboring the plasmid vector pFPV25. Data correspond to the average from three independent experiments.

Why Inefficient Translation of an Upstream ORF May Not Result in Transcriptional Polarity. Translation is thought to be a universal defense mechanism against Rho-dependent transcription termination because translating ribosomes protect an elongating RNAP from Rho invasion (5, 26). This is why disrupting the coupling of transcription with translation gives rise to transcriptional polarity, a process whereby compromised translation of a promoter-proximal ORF impairs transcription of downstream genes in the same transcription unit (12). For example, nonsense mutations in the first or second genes of the *gal* operon silence expression of the second or/and the third genes, respectively (27). Similarly, significant repression of tryptophanase expression due to constitutive Rho-dependent termination was observed when the start codon of the short ORF *tnaC* in the leader region of the tryptophanase *tnaAB* operon was replaced by a stop codon (28). By contrast, replacement of *mgtM*'s start codon with a stop codon derepressed the associated coding region (18).

Our data suggest that it is the particular arrangement of *rut*, RARE, and short ORF in a leader region that determines whether translation of the short ORF actually favors transcription elongation into the associated coding region instead of resulting in polarity. Rho-dependent transcription termination in the *mgtCBR* leader is actually stimulated by translation of the *mgtM* ORF (Fig. 6) because a ribosome translating *mgtM* favors a conformation in the *mgtCBR* RNA that sequesters RARE and allows Rho recruitment, thereby silencing the *mgtCBR* coding region (Fig. 5*B*). And in the case of the *tnaAB* leader, excess tryptophan induces ribosome stalling within *tnaC* in a manner uniquely dependent on the nascent TnaC peptide (29). A ribosome stalled at a Trp codon in the middle of *tnaC* occludes the *rut* site, thereby suppressing Rho-dependent termination.

RARE Inhibits Rho Function. Rho-dependent termination in the *mgtCBR* leader is modulated by RARE, an RNA element that hinders Rho function (Fig. 2*A*). RARE inhibits termination only when not sequestered in stem-loop B (Fig. 2*B*, Δ80–89 and insRARE). RARE does not affect Rho binding to the *mgtCBR* leader RNA (Fig. 3*B*), but it prevents formation of a catalytically competent complex (Fig. 3*A*).

The *mgtCBR* leader RNA with RARE single stranded adopts a conformation when bound to Rho that is distinct from that of the wild-type leader RNA (Fig. 4*C*). In the presence of Rho, RARE makes limited contact with the Rho-binding site: Δ80–89 RNA displays an RNase V1-sensitive site at positions 103–105 (Fig. 4*C*, blue bracket) followed by an RNase I-sensitive site at position 107 (Fig. 4*C*, green bracket), a pattern suggesting the presence of a hairpin. This pattern is in contrast to that displayed by the wild-type RNA in the presence of Rho: RNase V1-sensitive sites at positions 82–85, (Fig. 3*C*, blue dot) followed by RNase I- and lead acetate-sensitive sites at positions 90–92 (Fig. 4*C* and Fig. S2*C*). The former cleavage pattern was observed only in the presence of Rho, suggesting that base pairing between RARE and *rut* is unstable in the absence of Rho.

What is the fate of the complex formed by Rho and the *mgtCBR* leader RNA with single-stranded RARE? Kinetic and structural studies of Rho recruitment indicate that a Rho–RNA complex undergoes several isomerization events before reaching a translocation-competent state (Fig. S5) (30, 31). RARE might stabilize one of the intermediates on the recruitment pathway; for example, RARE might prevent the Rho ring from opening or closing, and in this way hinder Rho movement toward a paused RNAP (Fig. S5). Alternatively, changes in conformation of *rut* induced by RARE in the presence of Rho might affect Rho translocation at later steps. The idea that *rut* can participate in Rho-dependent termination postrecruitment is supported by the behavior of elongation factor NusG, which is particularly important for terminators with poor *rut* sites and affects RNA release in the process of Rho-dependent termination (5).

RARE differs from RNA or DNA signals that mediate antitermination by recruiting protein cofactors or modifying elongating RNAP (see ref. 32 for a review). This is because inhibition of Rho by RARE does not require cellular cofactors (Fig. S1*A*) or active transcription (Fig. 3*A* and Fig. S1*B*).

Sequence Elements Providing Specificity to Rho. Rho exerts a widespread effect in transcription (2, 33). Once Rho is recruited to a particular site on a nascent RNA, it is thought to translocate toward the transcribing RNAP. A translating ribosome or antitermination factors can shield the transcribing RNAP from interaction with Rho

(32, 33). Although these mechanisms contribute to Rho-dependent termination, independent lines of evidence indicate that they are not sufficient to explain Rho specificity.

First, genome-wide distribution of Rho-dependent termination revealed that Rho affects about 20% of nascent transcripts (1), whereas ChIP-chip data determined that Rho is associated with almost all nascent RNAs (13). In other words, only a fraction of transcripts that recruit Rho are subjected to Rho-dependent termination. Second, in vitro studies indicate that Rho can use RNA substrates that are very different from canonical Rho targets (34). Third, kinetic analysis of Rho's ATPase activity revealed that the process of hexamer ring opening, followed by RNA threading and ring closing, is a rate-limiting step in Rho recruitment (30). Fourth, structural studies demonstrated that RNA interactions with the Rho secondary binding site bring about major structural rearrangements within the protein ring (9, 35). And fifth, a study of transcription termination potency of various Rho mutants in vivo suggested that closure of the Rho hexamer around the substrate RNA serves as a regulatory point in Rho recruitment (31).

We propose that RARE represents a distinct class of RNA signal: one that suppresses Rho activity by inducing formation of a translocation-incompetent complex. This mode of action differs from those adopted by other Rho inhibitors (Fig. S5). For example, the YaeO protein prevents Rho from interacting with its RNA substrate (36), whereas processive antiterminators prevent RNA release by modifying elongating RNAP (32). Although both the Psu protein from bacteriophage P4 (37) and the antibiotic BCM (14) inhibit Rho's translocation, we believe that RARE operates by a different mechanism. The small size and location of RARE upstream of *rut* suggest that it likely contacts Rho nearby Rho's primary binding sites, whereas Psu binds at the opposite site of the Rho ring (37), and BCM binds deep inside the channel where it interferes with ATP binding (14, 38). Arrest of Rho-dependent termination by RARE is also distinct from regulation of Rho recruitment by alternative RNA structures that entrap *rut* (15) because the *mgtCBR* leader *rut* remained single stranded in either RNA conformation in the absence of Rho (Fig. 2*A*) and because RARE did not prevent Rho binding to its recruitment site (Fig. 3*B*). Moreover, once RARE was single stranded (Fig. 2*A*, insRARE), conformational changes in RNA had no effect on Rho-dependent termination (Fig. 6, UAA + insRARE, G54C + insRARE). Therefore, formation of alternative structures in the *mgtCBR* leader RNA serves merely as a means of modulating the availability of RARE. The proposed mechanism expressly allows RARE to determine which of the transcripts bound by Rho will be terminated.

Finally, our findings open the possibility of other RNA elements with similar properties to RARE existing in the bacterial transcriptome and modulating Rho specificity. The availability of RARE and RARE-like elements may be controlled by mechanisms other than formation of an RNA hairpin, including ribosome positioning, protein binding, a riboswitch, or a small RNA. Such elements may also affect the site of Rho-dependent termination when protecting the chromosome from R loops and double-strand breaks (39–41) and the suppression of pervasive antisense transcription (5).

Materials and Methods

Bacterial Strains, Plasmids, Oligodeoxynucleotides, Proteins, and Reagents. Bacterial strains and plasmids used in this study are listed in Dataset S1. Primers used in this study are listed in Dataset S2. *E. coli* strain DH5α was used as the host for preparation of plasmid DNA. Ampicillin was used at 50 μg/mL and kanamycin at 20 μg/mL. For in vivo experiments, wild-type *S. enterica* serovar Typhimurium 14028s (42) was used as the host strain. Bacteria were grown at 37 °C in LB broth or in N-minimal medium (pH 7.4) (43) supplemented with 0.1% casamino acids, 38 mM glycerol, and 10 μM of $MgCl_2$. One milliliter of the overnight culture was washed in the N-minimal medium without Mg^{2+} and resuspended in 1 mL of the same media. The suspended bacteria were inoculated 1/100 volume in N-minimal medium with 10 μM of $MgCl_2$ and ampicillin and grown for 4 h unless indicated otherwise. Fluorescence and OD_{600} of the cultures were measured in a Victor^3 plate reader from Perkin-Elmer. For the experiment involving BCM treatment, cells were harvested after 3 h of growth in N-minimal medium with 10 μM Mg^{2+} followed by a 15-min treatment with BCM added to the final concentration of 20 μg/mL. PCR reagents were from Invitrogen, [γ^{32}P]-ATP and [α^{32}P]-GTP, from Perkin-Elmer, and other chemicals from Sigma or Fisher. Plasmid DNAs and PCR products were purified using spin kits from Qiagen and Promega. RNAP was purified as described (44). Rho was purified as described in *SI Materials and Methods*.

Construction of Plasmids. Plasmid pAS69, carrying the *mgtCBR* leader sequence downstream of the λP_R promoter and a C-less initial transcribed sequence, was synthesized in vitro by GenScript USA based on vector pUC57; the full sequence is available upon request. Cloning was performed using modification enzymes from NEB as indicated in the plasmid description. Site-directed mutagenesis was performed using the Quikchange II kit from Agilent with plasmid pAS69 (used to generate templates for in vitro transcription) and pGFP303 (used for in vivo fluorescence measurements) and their derivative as templates and indicated oligonucleotides. See Dataset S1 for details.

Templates for in Vitro Transcription. Templates for pause and termination assays were generated by PCR amplification using primers 12230 and 13192, and plasmids pAS69 (wild-type), pAS75 (G54C), and pAS77 (G95C). Templates for RNA synthesis were generated by PCR amplification using primers 13347 and 13016, and plasmids pAS69 (wild type), pAS75 (G54C), pAS77 (G95C), pAS155 ([109–112]), pAS237 (Δ[80–89]), and pAS241 ([105–125]). Primers 14787/14788 were used for pYS1010-C145G (*mgtA* C145G) or pYS10116 (*mgtA* R1) and primers 15187/15188, for pFVP25 (*gfp* ORF).

Single-Round Pause Assay. Halted elongation complexes (designated A26 in Fig. 2*B*) were prepared with 50 nM of *E. coli* RNAP (core enzyme to σ^{70} ratio is 1:4) and 40 nM of linear DNA template prepared as described above, in Rho buffer [40 mM Tris·HCl pH 7.9, 50 mM KCl, 2 mM $MgCl_2$, 0.1 mM DTT, 3% (vol/vol) glycerol] supplemented with ApU (RiboMed) at 100 μM, ATP and UTP at 5 μM, GTP at 1 μM, and 5 mCi of [α^{32}P]-GTP (3000 Ci/mmol) during a 15-min incubation at 37 °C. Transcription was restarted by the addition of CTP, ATP, GTP, and UTP to 50 μM, and rifapentin to 25 μg/mL. Samples were removed at 15, 30, 45, 60, 120, 300, and 600 s and quenched by the addition of an equal volume of STOP buffer [95% (vol/vol) deionized formamide, 50 mM EDTA, 45 mM Tris-borate; pH 8.3, 0.1% bromophenol blue, 0.1% xylene cyanol]. For RNA sequencing, 10-μL aliquots of halted complexes were chased by 25 μM RNA sequencing mixtures (a single 3′OMeNTP at 1/10 to the corresponding rNTP) for 10 min and quenched by the addition of an equal volume of STOP buffer.

Samples were heated at 90 °C for 2 min and separated by electrophoresis in 6% denaturing acrylamide (19:1) gels (7 M urea, 0.5× TBE). RNA products were visualized and quantified using a PhosphorImager Storm 820 System (GE Healthcare), ImageQuant Software, and Microsoft Excel.

Rho-Dependent Termination Assay. Halted elongation complexes were prepared as described above. Transcription was restarted by the addition of GTP, CTP, ATP, and UTP to 1 mM, rifapentin to 25 μg/mL, and Rho to 20 nM where indicated. Reactions were carried out at 37 °C for 15 min and stopped as described above.

ATPase Assay. Rho ATPase activity was determined with the EnzCheck Phosphate Assay kit from Invitrogen as described (15) using RNA fragments corresponding to the *mgtCBR* leader or variants prepared as described in *SI Materials and Methods*.

Filter-Binding Assay. Determination of equilibrium K_d values for binding of RNAs to Rho was carried out by the nitrocellulose binding method (45). The 5′-end radiolabeled RNAs prepared as described in *SI Materials and Methods* were diluted to 0.01 nM in binding buffer [50 mM KCl, 1 mM $MgCl_2$, 20 mM Hepes pH 7.9, 3% (vol/vol) glycerol, 0.1 mM EDTA], heated to 80 °C for 3 min, and renatured at room temperature. To prevent nonspecific binding, yeast tRNA was added to 0.06 mg/mL. Samples were incubated with a series of dilutions of Rho prepared in binding buffer supplemented with 10% (vol/vol) glycerol and 4 mg/mL BSA, or storage buffer for 10 min at room temperature; the samples were filtered through 0.45-μm nitrocellulose filters (HAWP, Millipore) under vacuum; and the filters were washed with 5 mL of the binding buffer, air dried, and quantified using PhosphorImager and ImageQuant Software (GE Healthcare). To calculate the apparent equilibrium dissociation constants, the data were fit to a hyperbolic equation, $B = B_{max} \times [Rho]/([Rho] + K_d)$,

where B is a percentage of RNA bound, B_{max} is the maximum binding at infinite concentration of Rho, and K_d is the dissociation constant. The fitting was performed by nonlinear regression algorithm using Prism 6 (GraphPad Software). For each RNA–Rho combination, K_d measurements were independently repeated two to three times, and averages were calculated.

RNA Probing. The 5′-end radiolabeled RNAs prepared as described in *SI Materials and Methods* were diluted to 20 nM in Rho buffer, heated to 80 °C for 3 min, and renatured at room temperature. $MgCl_2$ was added to 5 mM and ATPγS [adenosine 5′-O(3-thiotriphosphate) from Calbiochem] to 2 mM. To prevent nonspecific binding, yeast tRNA was added to 0.05 mg/mL. Samples were incubated with 100 nM of Rho or equivalent volume of storage buffer at 37 °C for 3 min. For limited enzymatic digestion, 8-μL reaction aliquots were mixed with 2 μL of RNase T1 diluted to 0.3 units/μL, or RNaseI diluted to 0.3 units/μL, or RNase V1 diluted to 0.005 units/μL. Reactions were quenched by addition of 140 μL of 10 mM EDTA, and RNA was purified by phenol-chloroform extraction followed by ethanol precipitation. Pellets were resuspended in formamide loading buffer, loaded onto 6% (wt/vol) gel, and analyzed as described above.

Quantitative RT-PCR. Total RNA was isolated using RNeasy Kit (Qiagen) according to the manufacturer's instructions. The purified RNA was quantified using a NanoDrop machine (NanoDrop Technologies). cDNA was synthesized using High Capacity RNA-to cDNA Master Mix (Applied Biosystems). The mRNA levels of the *gfp* and *mgtC* genes were measured by quantification of cDNA using Fast SYBR Green PCR Master Mix (Applied Biosystems) and appropriate primers (*mgtC* coding: 7530/7531; *gfp*: 13725/13726) and monitored using a Fast ABI7500 machine (Applied Biosystems). Data were normalized to the levels of 16S ribosomal RNA amplified with primers 6970 and 6971.

ACKNOWLEDGMENTS. We thank Max Gottesman for providing bicyclomycin; Hubert Salvail for technical advice regarding the RNA probing experiments; Ronald Breaker for useful discussions; and Irina Artsimovitch, Paul Babitzke, Max Gottesman, Robert Landick, and Jeffrey Roberts for comments on the manuscript. This work was supported, in part, by NIH Grant AI49561 (to E.A.G., who is an investigator of the Howard Hughes Medical Institute).

1. Peters JM, et al. (2009) Rho directs widespread termination of intragenic and stable RNA transcription. *Proc Natl Acad Sci USA* 106(36):15406–15411.
2. Boudvillain M, Figueroa-Bossi N, Bossi L (2013) Terminator still moving forward: Expanding roles for Rho factor. *Curr Opin Microbiol* 16(2):118–124.
3. Yanofsky C, Ito J (1966) Nonsense codons and polarity in the tryptophan operon. *J Mol Biol* 21(2):313–334.
4. Newton WA, Beckwith JR, Zipser D, Brenner S (1965) Nonsense mutants and polarity in the *lac* operon of *Escherichia coli*. *J Mol Biol* 14(1):290–296.
5. Peters JM, et al. (2012) Rho and NusG suppress pervasive antisense transcription in *Escherichia coli*. *Genes Dev* 26(23):2621–2633.
6. Chen CY, Richardson JP (1987) Sequence elements essential for rho-dependent transcription termination at lambda tR1. *J Biol Chem* 262(23):11292–11299.
7. Skordalakes E, Berger JM (2003) Structure of the Rho transcription terminator: Mechanism of mRNA recognition and helicase loading. *Cell* 114(1):135–146.
8. Morgan WD, Bear DG, Litchman BL, von Hippel PH (1985) RNA sequence and secondary structure requirements for rho-dependent transcription termination. *Nucleic Acids Res* 13(10):3739–3754.
9. Skordalakes E, Berger JM (2006) Structural insights into RNA-dependent ring closure and ATPase activation by the Rho termination factor. *Cell* 127(3):553–564.
10. Burgess BR, Richardson JP (2001) RNA passes through the hole of the protein hexamer in the complex with the *Escherichia coli* Rho factor. *J Biol Chem* 276(6):4182–4189.
11. Richardson JP (2002) Rho-dependent termination and ATPases in transcript termination. *Biochim Biophys Acta* 1577(2):251–260.
12. Peters JM, Vangeloff AD, Landick R (2011) Bacterial transcription terminators: The RNA 3′-end chronicles. *J Mol Biol* 412(5):793–813.
13. Mooney RA, et al. (2009) Regulator trafficking on bacterial transcription units *in vivo*. *Mol Cell* 33(1):97–108.
14. Kohn H, Widger W (2005) The molecular basis for the mode of action of bicyclomycin. *Curr Drug Targets Infect Disord* 5(3):273–295.
15. Hollands K, et al. (2012) Riboswitch control of Rho-dependent transcription termination. *Proc Natl Acad Sci USA* 109(14):5376–5381.
16. Stewart V, Landick R, Yanofsky C (1986) Rho-dependent transcription termination in the tryptophanase operon leader region of *Escherichia coli* K-12. *J Bacteriol* 166(1):217–223.
17. Roberts JW, Shankar S, Filter JJ (2008) RNA polymerase elongation factors. *Annu Rev Microbiol* 62:211–233.
18. Lee EJ, Groisman EA (2012) Control of a *Salmonella* virulence locus by an ATP-sensing leader messenger RNA. *Nature* 486(7402):271–275.
19. Lee EJ, Choi J, Groisman EA (2014) Control of a *Salmonella* virulence operon by proline-charged $tRNA^{(Pro)}$. *Proc Natl Acad Sci USA* 111(8):3140–3145.
20. Lee EJ, Pontes MH, Groisman EA (2013) A bacterial virulence protein promotes pathogenicity by inhibiting the bacterium's own F_1F_o ATP synthase. *Cell* 154(1):146–156.
21. Snavely MD, Florer JB, Miller CG, Maguire ME (1989) Magnesium transport in *Salmonella typhimurium*: $^{28}Mg^{2+}$ transport by the CorA, MgtA, and MgtB systems. *J Bacteriol* 171(9):4761–4766.
22. Alix E, Blanc-Potard AB (2007) MgtC: A key player in intramacrophage survival. *Trends Microbiol* 15(6):252–256.
23. Hart CM, Roberts JW (1994) Deletion analysis of the lambda tR1 termination region. Effect of sequences near the transcript release sites, and the minimum length of rho-dependent transcripts. *J Mol Biol* 237(3):255–265.
24. Graham JE (2004) Sequence-specific Rho-RNA interactions in transcription termination. *Nucleic Acids Res* 32(10):3093–3100.
25. Groisman EA, et al. (2013) Bacterial Mg^{2+} homeostasis, transport, and virulence. *Annu Rev Genet* 47:625–646.
26. Boudvillain M, Nollmann M, Margeat E (2010) Keeping up to speed with the transcription termination factor Rho motor. *Transcription* 1(2):70–75.
27. Adhya SL, Shapiro JA (1969) The galactose operon of *E. coli* K-12. I. Structural and pleiotropic mutations of the operon. *Genetics* 62(2):231–247.
28. Stewart V, Yanofsky C (1986) Role of leader peptide synthesis in tryptophanase operon expression in *Escherichia coli* K-12. *J Bacteriol* 167(1):383–386.
29. Gollnick P, Yanofsky C (1990) $tRNA^{(Trp)}$ translation of leader peptide codon 12 and other factors that regulate expression of the tryptophanase operon. *J Bacteriol* 172(6):3100–3107.
30. Kim DE, Patel SS (2001) The kinetic pathway of RNA binding to the *Escherichia coli* transcription termination factor Rho. *J Biol Chem* 276(17):13902–13910.
31. Shashni R, Qayyum MZ, Vishalini V, Dey D, Sen R (2014) Redundancy of primary RNA-binding functions of the bacterial transcription terminator Rho. *Nucleic Acids Res* 42(15):9677–9690.
32. Santangelo TJ, Artsimovitch I (2011) Termination and antitermination: RNA polymerase runs a stop sign. *Nat Rev Microbiol* 9(5):319–329.
33. Washburn RS, Gottesman ME (2015) Regulation of transcription elongation and termination. *Biomolecules* 5(2):1063–1078.
34. Schwartz A, Walmacq C, Rahmouni AR, Boudvillain M (2007) Noncanonical interactions in the management of RNA structural blocks by the transcription termination rho helicase. *Biochemistry* 46(33):9366–9379.
35. Thomsen ND, Berger JM (2009) Running in reverse: The structural basis for translocation polarity in hexameric helicases. *Cell* 139(3):523–534.
36. Gutiérrez P, et al. (2007) Solution structure of YaeO, a Rho-specific inhibitor of transcription termination. *J Biol Chem* 282(32):23348–23353.
37. Ranjan A, Sharma S, Banerjee R, Sen U, Sen R (2013) Structural and mechanistic basis of anti-termination of Rho-dependent transcription termination by bacteriophage P4 capsid protein Psu. *Nucleic Acids Res* 41(14):6839–6856.
38. Skordalakes E, Brogan AP, Park BS, Kohn H, Berger JM (2005) Structural mechanism of inhibition of the Rho transcription termination factor by the antibiotic bicyclomycin. *Structure* 13(1):99–109.
39. Dutta D, Shatalin K, Epshtein V, Gottesman ME, Nudler E (2011) Linking RNA polymerase backtracking to genome instability in *E. coli*. *Cell* 146(4):533–543.
40. Washburn RS, Gottesman ME (2011) Transcription termination maintains chromosome integrity. *Proc Natl Acad Sci USA* 108(2):792–797.
41. Leela JK, Syeda AH, Anupama K, Gowrishankar J (2013) Rho-dependent transcription termination is essential to prevent excessive genome-wide R-loops in *Escherichia coli*. *Proc Natl Acad Sci USA* 110(1):258–263.
42. Fields PI, Groisman EA, Heffron F (1989) A *Salmonella* locus that controls resistance to microbicidal proteins from phagocytic cells. *Science* 243(4894 Pt 1):1059–1062.
43. Snavely MD, Miller CG, Maguire ME (1991) The *mgtB* Mg^{2+} transport locus of *Salmonella typhimurium* encodes a P-type ATPase. *J Biol Chem* 266(2):815–823.
44. Belogurov GA, et al. (2007) Structural basis for converting a general transcription factor into an operon-specific virulence regulator. *Mol Cell* 26(1):117–129.
45. Carey J, Cameron V, de Haseth PL, Uhlenbeck OC (1983) Sequence-specific interaction of R17 coat protein with its ribonucleic acid binding site. *Biochemistry* 22(11):2601–2610.
46. Zuker M (2003) Mfold web server for nucleic acid folding and hybridization prediction. *Nucleic Acids Res* 31(13):3406–3415.